

Influence of the GaN cap layer thickness on the two-dimensional electron gas (2-DEG) sheet charge density of GaN/AlInN/GaN HEMTs with polarization effect

A.Bellakhdar^{a,b,*}, A.Telia^b

^a*LMSF Laboratory of Semiconductors and Functional Materials, Amar Telidji University of Laghouat, Algeria*

^b*Laboratoire des Microsystèmes et Instrumentation LMI, Département d'Electronique, Faculté de Technologie, Université des Frères Mentouri, 2 Campus Ahmed Hamani, Ain El Bey, Constantine, Algeria*

In this study, GaN/AlInN/GaN high electron mobility transistor (HEMT) with various GaN cap layer thickness and with heavily n-doping GaN cap layer were presented. In order to investigate the effects of a GaN capping layer on performance of the (GaN/AlInN/GaN) heterostructures, a simple analytical model for the threshold voltage of GaN/AlInN/GaN high electron mobility transistor (HEMT) is proposed by solving one dimensional (1 D) Poisson equation, leads to find the relation between the two dimensional electron gas (2DEG) and the control voltage. Spontaneous and piezoelectric polarizations at AlInN/GaN and GaN/AlInN interfaces have been incorporated in the analysis. Our simulations indicate that the GaN cap layer reduces the sheet density of the two dimensional electron gas (2DEG), leading to a decrease of the drain current, and that n+ doped GaN cap layer provides a higher sheet density than undoped one.

(Received November 28, 2021; Accepted February 19, 2022)

Keywords: GaN cap, GaN/AlInN/GaN HEMT, 2DEG, 2DHG, Spontaneous polarizations, Piezoelectrics polarizations

1. Introduction

Recently, AlInN / GaN High electron mobility transistors (HEMT) devices, based on III-nitride wide band gap semiconductors, are of increasing interest due to their enormous potential and excellent performance demonstrated in high power and high frequency applications [1,2]. This is due to their superior properties in terms of high breakdown voltage, and high carrier density and mobility [3]. AlInN/GaN heterostructure show better performance than conventional AlGaIn/GaN heterostructure devices. Lattice mismatch AlInN/GaN provides strong polarization field that leads to a large conduction band bending at the hetero-junction interface. This creates a high sheet carrier concentration, above 10^{13} cm^{-2} , at the interface without intentionally doping, compared with other III-V compound semiconductor based devices [4,5] and also avoids the problem of interface and bulk defects occurring in AlGaIn/GaN structures with high Al content, due to strain relaxation [6]. However, the AlInN alloy can be lattice-matched to GaN with 17% of In and 83% of Al content [7]. In the lattice-matched $\text{Al}_{0.83}\text{In}_{0.17}\text{N}/\text{GaN}$ heterostructure, there is no mechanical constrains in the epitaxial structures, which reduces strain-defects related relaxation problems. Moreover, higher sheet charge density can be induced by the large spontaneous polarization even without contribution from piezoelectric polarization compared to the conventional AlGaIn/GaN HEMTs [1],[8].

Various layers and channel alternatives are used in nitride-based HEMTs in order to improve the performance of devices . The use of the GaN cap layer in the GaN -based heterostructures is presented by various studies in the literature.

* Corresponding author: as.bellakhdar@lagh-univ.dz
<https://doi.org/10.15251/DJNB.2022.171.233>

Recently, In ordre to investigate the effect of the GaN cap layer on the performance of these devices, Heikman et al.[9] and Asgari et al.[10] have proposed a GaN/Al_{0.32}Ga_{0.68}N/GaN heterostructure deposited on a saphir substrate, and they show that the sheet carrier density decreases with thicker cap layers while the mobility increases. Similar effects were reported by Peng Cui et al [11] and Tao et al [12] for an AlN/GaN heterostructure. Also a heavily doped n-GaN cap layer has been employed to improve high-frequency performance and to reduce access and ohmic contact resistances. To maximize the high frequency performance of AlGaIn HEMTs, Green et al [13] incorporated GaN cap layers in GaN/AlGaIn/GaN structures by heavily n-doping the upper GaN layer; thus parasitic contact resistances were greatly reduced. On the other hand, An activated P-GaN cap layers in AlGaIn/GaN HEMTs used by Li et al [14] improve the breakdown characteristics and reduce the leakage current. A study by P.Kordos et al [15] showed that a thick undoped GaN cap layer reduce the gate leakage and the devices on doped GaN/AlGaIn/GaN structure show improved DC and RF performance.

Finally, The GaN capped HEMTs have some advantages over conventional HEMTs with no caps such as smaller surface roughness, smaller gate leakage current, higher breakdown voltage, higher sheet carrier density, and smaller contact resistance in case of doped caps [16].

In this paper, we present analytical models for threshold voltage, 2-D electron gas density (2DEG) n_s and the I-V characteristics of these HEMTs with a doped n-GaN cap layer. We study the n+GaIn/AlInN/GaN structures, with and without GaN cap layer and we investigate the effect of the GaN cap layer on threshold voltage, sheet carrier density, and current voltage characteristics. Spontaneous and piezoelectric polarization-induced charges have been also considered. The results are in good agreement with the existing experimental data reported in the literature.

2. Theory and modeling

2.1. Device structure

In our proposed device shown in figure 1, the studied structure is GaN/Al_{0.83}In_{0.17}N/GaN.

The layer sequence, from top to bottom, it consist of thin GaN cap layer of thickness d_{cap} . this one could be undoped or heavily n+doped with Silicium to a concentration equal to $1 \times 10^{20} \text{ cm}^{-3}$, an undoped Al_{0.83}In_{0.17}N additional layer of thickness d_a , an n-doped Al_{0.83}In_{0.17}N thick barrier layer of thickness d_b and doping concentration N_D provides the 2DEG sheet charge density, an undoped Al_{0.83}In_{0.17}N spacer layer of thickness d_s prevents impurity scattering from the n+GaN cap to the n- Al_{0.83}In_{0.17}N layer [17], which increases the density and mobility of carriers in the channel, and an undoped GaN thick buffer layer deposited over a (SiC, Si or Saphir) substrate. The 2DEG channel appears at the interface between the buffer layer and the undoped Al_{0.83}In_{0.17}N spacer layer. Two-Dimensional Electrons Gas (2DEG) is the channel formed in a quantum well from electrons accumulation along a heterojunction of Al_{0.83}In_{0.17}N/GaN HEMT.

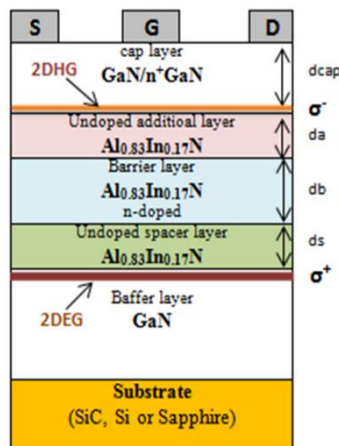


Fig 1. Cross-sectional structure of GaN/Al_{0.83}In_{0.17}N/GaN.

The GaN cap layer on top of the hetero-structure raises the conduction band ΔE_C and produces a large enhancement in effective barrier height E_{beff} . This is due to a negative polarization charge ($-\sigma$) at the upper hetero-interface, which increases the electric fields in the barrier layer, and hence decreases the 2DEG density, leading to a reduction in the gate leakage current [14]. When the GaN cap becomes thicker, the charge density in the channel is smaller; the valence-band ΔE_V of the GaN cap shifts upward, and the valence band eventually reaches the Fermi level E_F . At this point, a two-dimensional hole gas (2DHG) is formed at the upper GaN/AlInN interface (Fig. 2.b) [11]. The n-doping of the GaN is also advantageous as it reduces the contact resistance [18]. The band diagram and charge distribution in Fig.2 (a,b) and Fig.3 respectively show the formation of the two dimensional electron gas (2DEG) and two-dimensional hole gas (2DHG) in GaN/AlInN/GaN heterostructures induced by polarization, the dashed line corresponds to the doped GaN cap, while the continuous line is for the undoped case.

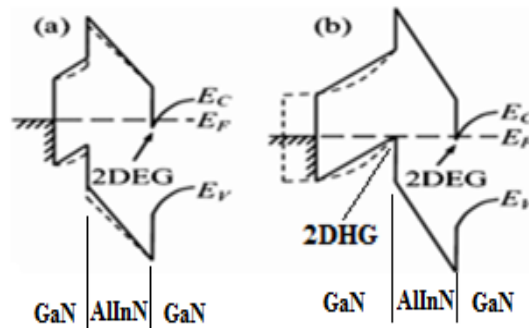


Fig. 2. (a,b) Band diagrams of GaN/AlInN/GaN HEMT; (a) GaN/AlInN/GaN HEMT heterostructures with a thin or (b) thick GaN capping layer.

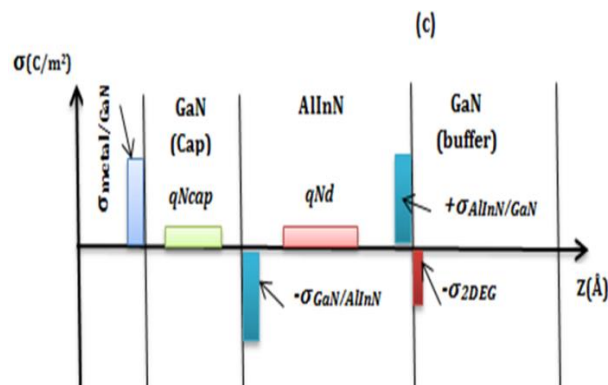


Fig. 3. Charge distribution of GaN/AlInN/GaN HEMT.

The description and electrical parameter values used for model development and simulation of the device characteristics are listed in Table 1.

Table 1. Electrical parameters of the structure used in the simulation.

Parameter (units)	Description	Values
R_s (Ω)	parasitic source resistance	0.3
R_d (Ω)	parasitic drain resistance	0.3
μ_0 ($cm^2/V.s$)	low field mobility	900×10^{-4}
N_{cap} (cm^{-3})	n+GaN cap doping density	1×10^{20}
N_d (cm^{-3})	Barrier doping concentration	1×10^{18}
E_c (V/m)	critical electric field	190×10^5
v_{sat} (m/s)	saturation velocity	2.1×10^5
L (μm)	gate length	1
W (μm)	gate width	100
d_{cap} (nm)	GaN cap layer	1,3,5
d_a (nm)	additional layer	3
d_b (nm)	barrier layer	20
d_s (nm)	spacer layer	3

The physical parameters for $Al_mIn_{(1-m)}N$ that depend on the Al mole fraction m are listed in Table 2, in which their expressions versus m are given[19, 20-22].

Table 2. Material parameters for $Al_mIn_{(1-m)}N$ used in the calculation [19, 20-22].

Parameters/ units	Description	Expression
$C_{13}(m)$ (GPa)	elastic constant	$24m + 70$
$C_{33}(m)$ (GPa)	elastic constant	$172m + 205$
$e_{31}(m)$ (Cm-2)	piezoelectric constant	$-0.12m - 0.21$
$e_{33}(m)$ (Cm-2)	piezoelectric constant	$0.69m + 0.81$
$a(m)$ (\AA)	lattice constant	$(-0.4753m + 3.5848)$
$P_{Sp}(m)$ (Cm-2)	spontaneous polarization	$-0.048m - 0.042$
$\epsilon_{AlInN}(m)$ (cm-1V-1)	dielectric constant	$(-4.3m + 14.21) 8.854 \times 10^{-12}$
$e\Phi(m)$ (eV)	Ni Schottky barrier	$1.94m + 0.2$
$E_g(m)$ (eV)	energy band gap	$6.28 m + 0.7(1-m) - 3.1 m(1-m)$
$\Delta Ec(m)$ (eV)	band discontinuity	$0.63 E_g(m) - E_g(0)$

2.2. Threshold voltage model

The threshold voltage V_{th} is an essential quality control parameter of the HEMT in the assessment of its reliability [23]. It is defined as the applied gate voltage for which the channel is completely depleted, and is considered as the minimum potential in the channel [24]. The analytical calculation of the threshold voltage leads us to find the relationship between the sheet charge density 2DEG n_s and the control voltage V_{gs} . For this; we use the one-dimensional Poisson equation which relates the charge distribution and the voltage V_{gs} : The Poisson equation is written as:

$$\frac{d^2V(z)}{dz^2} = -\frac{\rho(z)}{\epsilon_{GaN}} = -\frac{qN_{cap}}{\epsilon_{GaN}} \quad (1)$$

where: $\rho(z)$ is the charge density, ϵ_{GaN} is the dielectric constant of GaN, q is the elementary charge, $V(z)$ is the electrostatic potential, and N_{cap} is a GaN cap doping density. The dependence

of V_{th} on Al mole fraction m including the effects of both spontaneous and piezoelectric charge polarization, in a doped n+GaN cap layer is given by the following expressions:

$$V_{th}(m) = -\frac{qN_{cap}d_{cap}^2}{2\epsilon_{GaN}} - \frac{qN_d d_b}{\epsilon_{AlInN}(m)} \left(d_a + \frac{d_b}{2} + \frac{\epsilon_{AlInN}(m)}{\epsilon_{GaN}} d_{cap} \right) + \frac{E_{Schottky}}{q} + \frac{E_F}{q} - \frac{\sigma^-(m)d_{cap}}{\epsilon_{GaN}} - \frac{\sigma^+(m)d}{\epsilon_{AlInN}(m)}, \quad (2)$$

where:

$$d = \frac{\epsilon_2(m)}{\epsilon_1} d_{cap} + d_1, \quad \text{and} \quad d_1 = d_s + d_b + d_a + \Delta d$$

d is the distance between the gate and the channel without GaN cap layer, $\epsilon_{AlInN(m)}$ and ϵ_{GaN} are the dielectric constants of $Al_mIn_{(1-m)}N$ and GaN respectively, q is the electronic charge, $E_{Schottky}$ represents the Schottky-barrier height between the metal and the AlInN layer in bare structures and between the metal and GaN in capped structures, E_F is the Fermi level assuming ΔE_F at 300°K [21], and σ is the polarization induced charge density at the interface (see Fig. 2 and Fig.3).If σ is positive, free electrons will tend to compensate for the polarization induced charge and will form a 2DEG. On the other hand, a negative sheet charge density causes an accumulation of holes, leading to a 2DHG at the interface [25].

2.3. Two dimensional electron gas 2DEG charge density model

The Two dimensional electron gas density n_s is one of the principal entities governing the performance and operation of AlInN/GaN HEMT devices [26]. For AlInN/GaN heterostructure, The 2DEG sheet carrier density can be calculated from the solution of Schrodinger's and Poisson's equations in the quantum well, considering the first two sub-bands in the GaN conduction band. A self-consistent solution of n_s can be expressed as [21, 27-28]:

$$n_s(E_F) = Dk_B T \ln \left(\left(1 + \exp \left(\frac{E_F - E_0}{k_B T} \right) \right) \times \left(1 + \exp \left(\frac{E_F - E_1}{k_B T} \right) \right) \right) \quad (3)$$

where: $E_0 = \gamma_0 n_s^{2/3}$ (eV) and $E_1 = \gamma_1 n_s^{2/3}$ (eV) are the allowed energy levels in the quantum well. $\gamma_0 = 2.123 \times 10^{-12}$ and $\gamma_1 = 3.734 \times 10^{-12}$ with $D = (4\pi m^*/h^2)$ is the conduction band density of state of the 2DEG system, k_B is the Boltzmann constant, m^* is the electron effective mass, h is Planck constant. T is the ambient temperature. When a gate voltage V_{gs} is applied through a Schottky contact, the sheet carrier density n_s , under strong inversion region in the channel formed at the AlInN/GaN interface, at an arbitrary point x along the channel, with considering spontaneous and piezoelectric polarization [29] is given by:

$$n_s(m, x) = \frac{2qD \epsilon_{AlInN}(m)}{\epsilon_{AlInN}(m) + 2q^2 D d} \times (V_{gs} - V_{th}(m) - V_c(x)) \quad (4)$$

where: $V_{th}(m)$ is the threshold voltage (see II-2), $V_c(x)$ is the channel potential at any point x along the channel due to the applied drain voltage, V_{gs} is the gate-to-source bias voltage. In a HEMT, the sheet carrier density in the 2DEG channel is modulated by the application of negative bias (mode normally-on) to a Schottky metal gate in order to deplete the electron channel. In our simulation, we use a (nickel) Ni Schottky barrier contact at the surface.

2.4. Polarization-induced sheet charge density

In III-Nitride heterostructures, the difference in the spontaneous and piezoelectric polarization between two different layers would result in a fixed sheet of polarization charge at the interface. This charge tends to attract high concentration of electrons or holes depending on the net polarization at the interface [30].

At an abrupt interface of a top/bottom layer (GaN/AlInN or AlInN/GaN heterostructures), the polarization can decrease or increase within a bilayer, causing a fixed polarization sheet charge density defined [31] by:

$$\begin{aligned}\sigma(P_{SP} + P_{PZ}) &= P_{bottom} - P_{top} = (P_{bottom}^{SP} + P_{bottom}^{PZ}) - (P_{top}^{SP} + P_{top}^{PZ}) \\ &= (P_{bottom}^{PZ} - P_{top}^{PZ}) + (P_{bottom}^{SP} - P_{top}^{SP}) = \sigma(P_{PZ}) + \sigma(P_{SP})\end{aligned}\quad (5)$$

The Quantum Well (QW) at the heterointerface confines electrons or holes in a direction perpendicular to the interface. For a net positive polarization at the interface this confinement results into two dimensional electron gas 2DEG and for a net negative polarization, this results into two dimensional holes gas (2DHG) [30]. The direction of the polarization-induced field formed at the lower AlInN/GaN interface ($+\sigma$) is opposite to that in the upper GaN/AlInN one ($-\sigma$) (Figs. 2 and 4). Then, the conduction band is rising as shown in Fig. 2. Therefore 2DEG and 2DHG appear at the AlInN/GaN and GaN/AlInN interfaces respectively, as shown in Figure 4.

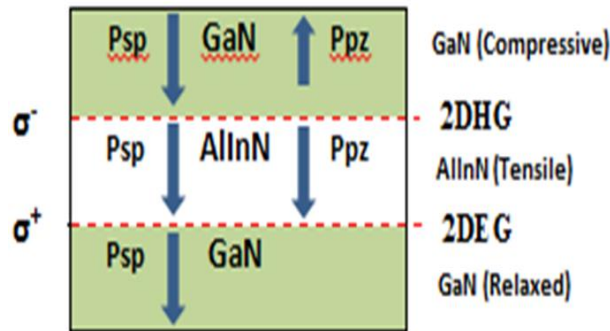


Fig. 4. Polarization -induced sheet charge density and direction of the spontaneous and piezoelectric polarization in GaN/AlInN and AlInN/GaN heterostructures.

For the AlInN/GaN or GaN/ AlInN HEMT, the total positive polarization charge density can be given by the sum of the piezoelectric P_{PZ} and spontaneous P_{SP} polarizations respectively, which induce a sheet charge density σ at the hetero-interfaces [19]:

$$P_{Al_m In_{(1-m)} N} = P_{Al_m In_{(1-m)} N}^{SP} + P_{Al_m In_{(1-m)} N}^{PZ} . \quad (6)$$

At the lower interface of the heterostructures, the total polarization can change abruptly, which creates a fixed polarization charge σ defined by:

$$\sigma^+(m) = \sigma_{Al_m In_{(1-m)} N / GaN} = P_{GaN} - P_{Al_m In_{(1-m)} N} = (P_{GaN}^{SP} + P_{GaN}^{PZ}) - (P_{Al_m In_{(1-m)} N}^{SP} + P_{Al_m In_{(1-m)} N}^{PZ}) . \quad (7)$$

Similarly, at the upper interface of the hetero-structure, the charge density is:

$$\sigma^-(m)_{\text{GaN}/\text{Al}_m\text{In}_{(1-m)}\text{N}} = -\sigma^+(m)_{\text{Al}_m\text{In}_{(1-m)}\text{N}/\text{GaN}}. \quad (8)$$

Thus the net polarization induced sheet charge density at AlInN/GaN interface is given by:

$$\sigma(m) = \left| P_{\text{Al}_m\text{In}_{(1-m)}\text{N}}^{\text{PZ}} + P_{\text{Al}_m\text{In}_{(1-m)}\text{N}}^{\text{SP}} - P_{\text{GaN}}^{\text{SP}} \right|. \quad (9)$$

with: $P_{\text{GaN}}^{\text{SP}} = -0.029(\text{C} / \text{m}^2)$

The expression for piezoelectric polarization can be expressed as:

$$P_{\text{Al}_m\text{In}_{(1-m)}\text{N}}^{\text{PZ}} = 2 \frac{a(0) - a(m)}{a(m)} \left[e_{31}(m) - e_{33}(m) \frac{C_{31}(m)}{C_{33}(m)} \right]. \quad (10)$$

all these values of the nitrides interesting for this work are shown in table II.

2.5. Current-voltage characteristics

The drain current induced by a two-dimensional gas of electrons 2DEG of the HEMT transistor based AlInN /GaN heterostructure can be expressed from the current density equation presented in [27], where temperature effects are included in the electron mobility:

$$I_{ds}(T, m) = wq\mu(T, x) \times \left(n_s(m, x) \frac{dV_C(x)}{dx} + \frac{k_B T}{q} \frac{dn_s(m, x)}{dx} \right), \quad (11)$$

where $\mu(T, x)$ is the temperature dependent mobility, whose expression is given in [32]:

$$\mu(T, x) = \frac{\mu_o(T)}{1 + \frac{1}{E_1} \frac{dV_C(x)}{dx}}, \quad (12)$$

with:

$$E_1 = \frac{E_c v_{sat}}{\mu_o(T) E_c - v_{sat}} \quad (13)$$

Substituting expressions (4) and (12) in (11), and integrating along the channel leads to [33,34]:

$$I_{ds}(m) = \frac{-\alpha_2(m) + \sqrt{\alpha_2^2(m) - 4\alpha_1(m)\alpha_3(m)}}{2\alpha_1(m)}. \quad (14)$$

with:

$$\left\{ \begin{array}{l} \alpha_1(m) = (2R_s + R_d) \left(\frac{\mu_0 E_c - v_{sat}}{E_c v_{sat}} - \frac{w \mu_0 q^2 D \varepsilon_{AlInN}(m) R_d}{2q^2 D (d_z) + \varepsilon_{AlInN}(m)} \right), \\ \alpha_2(m) = -L - \frac{\mu_0 E_c - v_{sat}}{E_c v_{sat}} V_{ds} + \frac{2w \mu_0 q^2 D \varepsilon_{AlInN}(m)}{2q^2 D (d_z) + \varepsilon_{AlInN}(m)} \\ \quad \times \left(V_{ds} (R_s + R_d) - V_{gs}'(m) (2R_s + R_d) \right), \\ \alpha_3(m) = \frac{2w \mu_0 q^2 D \varepsilon_{AlInN}(m)}{2q^2 D (d_z) + \varepsilon_{AlInN}(m)} \times V_{ds} \left(V_{gs}'(m) - \frac{V_{ds}}{2} \right), \end{array} \right.$$

and

$$V_{gs}'(m) = V_{gs} - V_{th}(m) - \frac{k_B T}{q}.$$

V_{ds} is the drain-to-source voltage. Note that, for the sake of simplicity, the dependence on T and/or m of the coefficients Ai , μ_0 and ε has not been written down in the preceding expressions and will not be from now on. The low-field mobility μ_0 depends on the electron concentration $n_s(m)$, which further depends on the doping concentration, on the temperature and on the material quality.

3. Results and discussion

Figure 5. shows the influence of the barrier thickness on the sheet carrier density in $Al_{0.83}In_{0.17}N/GaN$. For the structure, the sheet density increases rapidly for barriers thinner than 10 nm and then tends to saturate, with a higher saturation value ($30 \times 10^{12} \text{ cm}^{-2}$ around 40 nm). Our model is in excellent agreement with the experimental data (circles in Figure. 5) extracted from the literature [7]).

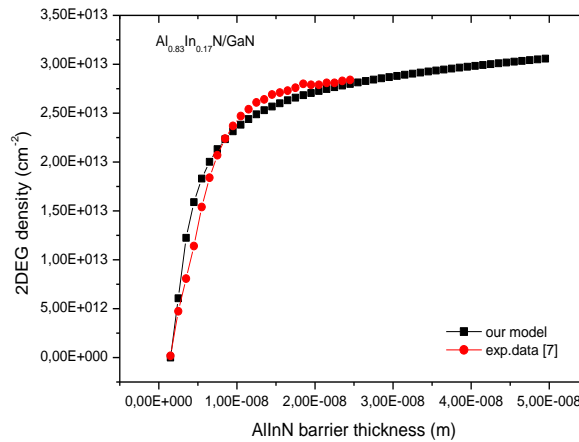


Fig. 5. Comparison of modeled 2DEG sheet density as a function of AlInN barrier thickness for $Al_{0.83}In_{0.17}N/GaN$ structure with experimental data [7].

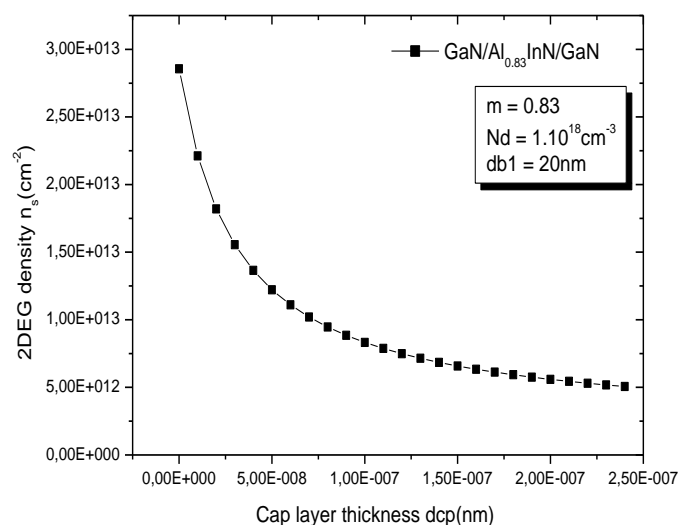


Fig. 6. Variation of 2DEG sheet density for GaN/Al_{0.83}In_{0.17}N/GaN HEMTs as a function of the GaN capping layer thickness.

As shown in Figure.6, the sheet carrier density is plotted as a function of the GaN cap layer thickness. The sheet carrier density decreases monotonously when the cap layer becomes thicker and remains almost constant for thick cap layers ($\sim 5.2 \times 10^{12} \text{ cm}^{-2}$ for GaN/Al_{0.83}In_{0.17}N/GaN structure, over 25 nm).

Figure.7 shows that GaN/Al_{0.83}In_{0.17}N/GaN HEMTs with an undoped GaN cap layer exhibit a smaller sheet density than with a n+doped GaN cap layer. The reduction of 2DEG sheet density may be attributed to the additional negative polarization charges formed at the interface between GaN and AlInN. The sheet carrier density increases slightly with the barrier thickness. On the other hand, the 2DEG sheet density is much higher in n+GaN/AlInN/GaN structure. This improvement is attributed to a better electron confinement in the channel due to a larger electric field, arising firstly from higher spontaneous polarization charge at the GaN/Al_{0.83}In_{0.17}N/GaN heterointerface, and secondly from the conduction band discontinuity formed at the interface.

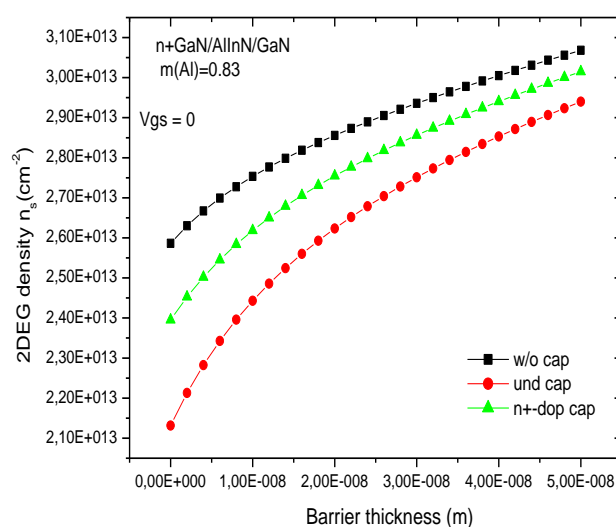


Fig. 7. Variation of 2DEG density as a function of barrier thickness for n+GaN/Al_{0.83}In_{0.17}N/GaN, without, and with undoped and n+doped GaN cap layer. Here $V_{gs} = 0 \text{ V}$.

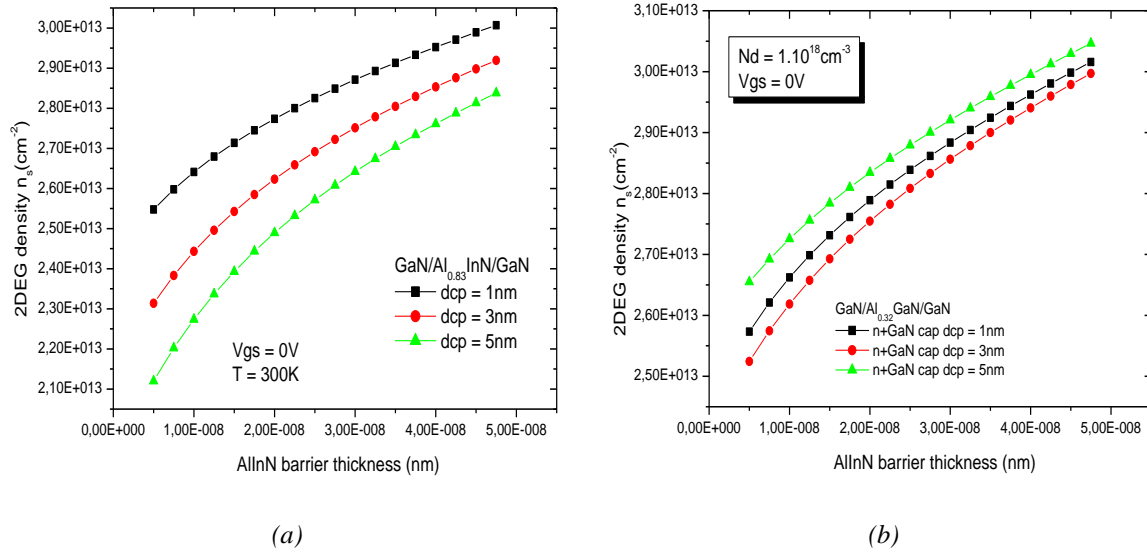


Fig 8. Variation of 2DEG sheet density as a function of AlInN barrier thickness for GaN/ Al_{0.83}In_{0.17}N /GaN heterostructures with various valous of (a) undoped and (b) n+doped GaN cap layer thickness. Here $V_{gs} = 0$ V.

Figure 8. shows the variation of the 2DEG sheet density as a function of the AlInN barrier thickness, for different thicknesses d_{cap} of undoped (Figure. 8.a) and n+doped (Figure. 8.b) GaN cap layers. Let us notice that the variation of 2DEG sheet density for various values d_{cap} is significant, especially for undoped GaN caps. It was reported that increasing the thickness of GaN cap layer would reduce the electron density in 2DEG channel [35].The 2DEG sheet density decreases when the undoped GaN cap layer becomes thicker. This is explained by the contribution of the heavily doping cap layers in the case of higher thicknesses and by the large spontaneous polarization charge at the GaN/ Al_{0.83}In_{0.17}N /GaN heterointerface.

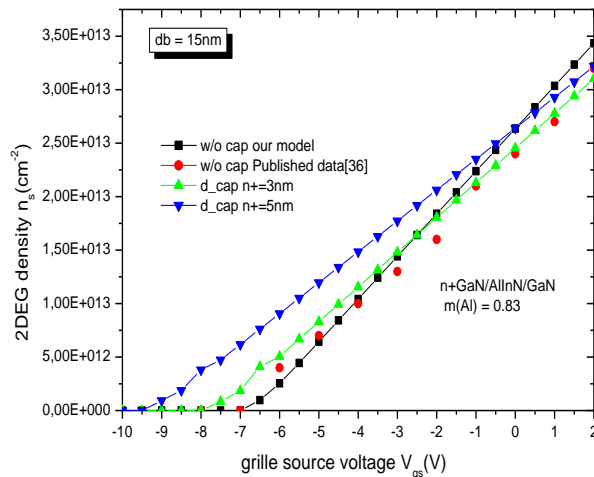


Fig. 9.Variation of sheet carrier density as a function of grille source voltage with different n+dopedGaN cap layer thickness and without GaN cap layer for n+GaN/ Al_{0.83}In_{0.17}N /GaN. $V_{gs} = 0$.

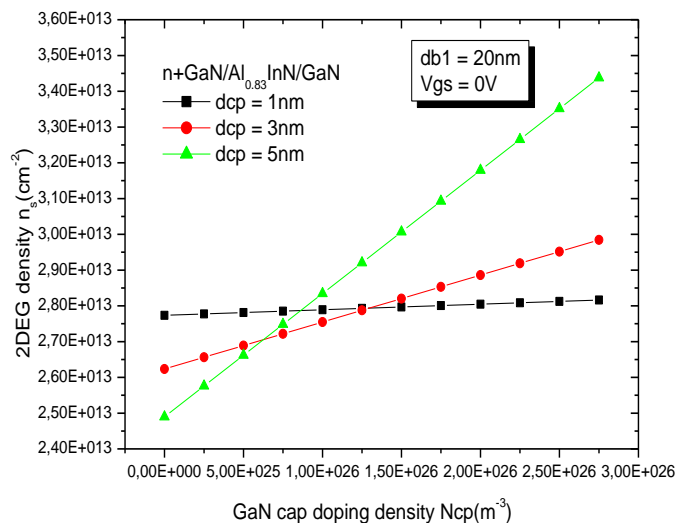


Fig. 10. Variation of sheet carrier density as a function of GaN cap doping density with different GaN cap layer thickness for GaN/Al_{0.83}In_{0.17}N/GaN structure.

The variation of the sheet carrier density n_s as a function of gate source voltage V_{gs} is presented in Figure.9 for different thicknesses of the n+doped GaN cap layer. n_s increases almost linearly with V_{gs} over a given threshold. Consequently, the depth of the potential well at heterointerface decreases, as well as the 2DEG density[34]. Moreover, the curves shift to more negative V_{gs} when increasing the n+doped GaN cap layer thickness, which indicates a simultaneous decrease of the threshold voltage V_{th} . Full circles are published data from [36].

The variation of sheet carrier density n_s is plotted in figure 10 versus the cap layer doping density N_{cap} . As expected, it increases proportionally to N_{cap} . Moreover, the variation is stronger when increasing the cap thickness. Typically, with a 5 nm cap thickness, n_s in n+GaN/AlInN/GaN structure increases in $2.5 \times 10^{13} \text{ cm}^{-2}$ for an undoped GaN cap layer ($N_{cap} = 0$) to $3.45 \times 10^{13} \text{ cm}^{-2}$ for $N_{cap} = 2.75 \times 10^{20} \text{ cm}^{-3}$. This improvement is explained by the additional contribution of heavily doping cap layer of higher thickness and large spontaneous polarization charge.

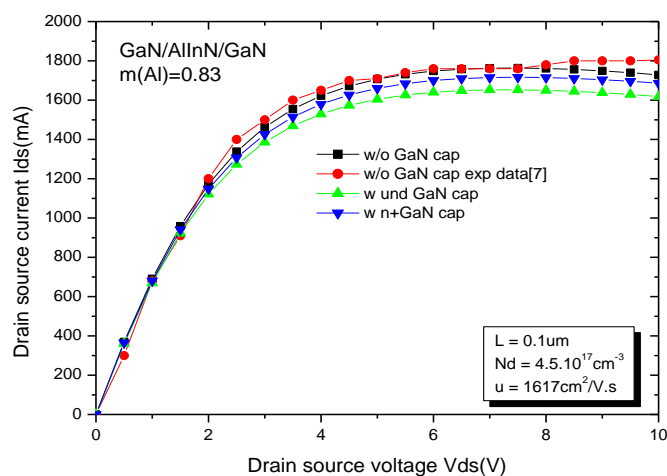


Fig. 11. Variation of drain source current as a function of drain source voltage with undoped, n+doped and without GaN cap layer at gate voltage $V_{gs} = 0V$ for GaN/AlInN/GaN structure., $db = 30 \text{ nm}$.

The drain current is diminished in structure covered with an undoped GaN cap layer, as seen in Figure.11. This can be explained by the reduction of the 2DEG sheet density due to the additional negative polarization charges formed at the interface between GaN and AlInN. The drain current is more intense. Also, it is seen that the drain current increases linearly with small values of V_{ds} and then saturates at higher V_{ds} because of the very high sheet charge density, resulting from large conduction band discontinuity and strong polarization effects. The model gives good agreement with the result of Ref [7].

4. Conclusion

In this work, we have studied the effect of GaN cap layer thickness on the two-dimensional electron gas (2-DEG) sheet charge density for GaN/AlInN/GaN HEMT. In this case a simple analytical model for the threshold voltage of GaN/ AlInN /GaN high electron mobility transistor (HEMT) is proposed by solving one dimensional (1 D) Poisson equation, leads to find the relation between the two dimensional electron gas (2DEG) and the control voltage, taking into account the effect of spontaneous and piezoelectric polarizations at AlInN/GaN and GaN/AlInN interfaces. We have presented a comparative study of the effect of doped and undoped GaN capping layer on the two dimensional electron gas (2DEG) of this HEMT.

It has been found that the deposition of an undoped GaN cap layer on top AlInN/GaN reduces the sheet carrier concentration, proportionally to the cap layer thickness, and makes the drain current decreasing. This is due to a negative polarization charge at the upper hetero-interface, which increases the electric fields in the barrier layer, and hence decreases the 2DEG density. Also n+doping the GaN cap layer leads to similar but more pronounced effects, the sheet density becomes higher. This improvement is attributed to a better electron confinement in the channel due to electric field arising from higher spontaneous polarization charge at the n+GaN/AlInN/GaN hetero-interface and by a larger conduction band discontinuity formed at the same interface. Close proximity with experimental data given in the literature confirms the validity of the proposed model.

References

- [1] G. Amarnath, D. K. Panda, T. R. Lenka, *Int J Numer Model.* 32(6), e2456 (2018); <https://doi.org/10.1002/jnm.2456>
- [2] H. M. Mahmood, M. A. Abdullah, A. Ramizy, A. S. Mohammed, *Digest Journal of Nanomaterials and Biostructures* 15(2), 587 (2020).
- [3] S. Ghosh, A. Dasgupta, S. Khandelwal, S. Agnihotri, Y. S. Chauhan, *IEEE Trans Electron Dev* 62(2), 443 (2015); <https://doi.org/10.1109/TED.2014.2360420>
- [4] F. Medjdoub, D. Ducatteau, C. Gaquiere, J.-F. Carlin, M. Gonschorek, E. Feltin, *Electronics Letter* 43(5), 71(2007); <https://doi.org/10.1049/el:20073170>
- [5] L. Bo, F. Zhihong, Z. Sen, D. Shaobo, Y. Jiayun, L. Jia, W. Jingjing, Z. Xiaowei, F. Yulong, C. Shujun, *Journal of Semiconductors* 32(12), (2011).
- [6] Hemant Pardeshi, Godwin Raj, Sudhansu Pati, N. Mohankumar, Chandan Kumar Sarkar, *Superlattices and Microstructures* 60, 47 (2013); <https://doi.org/10.1016/j.spmi.2013.04.015>
- [7] S. Guo, X. Gao, D. Gorka, J. W. Chung, H. Wang, T. Palacios, A. Crespo, J. K. Gillespie, K. Chabak, M. Trejo, V. Miller, M. Bellot, G. Via, M. Kossler, H. Smith, D. Tomich, *Phys. Status Solidi A* 207(6), 1348 (2010); <https://doi.org/10.1002/pssa.200983621>
- [8] Lianhong Yanga, Baohua Zhanga, Yanqing Lia, Dunjun Chena, *Materials Science in Semiconductor Processing* 74, 42 (2018).
- [9] S. Heikman, S. Keller, Y. Wu, J. S. Speck, S. P. DenBaars, U. K. Mishra, *J. Appl. Phys.* 93, 10114 (2003); <https://doi.org/10.1063/1.1577222>
- [10] A. Asgaria, M. Kalafia, L. Faraone, *Physica E* 25, 431 (2005); <https://doi.org/10.1016/j.physe.2004.07.002>
- [11] Peng Cui et al, *Superlattices and Microstructures* 100, 358 (2016); <https://doi.org/10.1016/j.spmi.2016.09.039>
- [12] Z.J. Tao, Z.-J. Lin, C.-B. Luan, Y.-J. Lu, Z.-H. Feng, M. Yang, *Chin. Phys. B* 23(12), 127104 (2014); <https://doi.org/10.1088/1674-1056/23/12/127104>
- [13] R. T. Green, I. J. Luxmoore, K. B. Lee, P. A. Houston, F. Ranalli, T. Wang, P. J. Parbrook, M. J. Uren, D. J. Wallis, T. Martin, *J. Appl. Phys.* 108, 013711 (2010); <https://doi.org/10.1063/1.3457356>
- [14] C-H. Li, Y-C. Jiang, H-C. Tsai, Y-N. Zhong, Y-M. Hsinz, *ECS Journal of Solid State Science and Technology* 6(11), S3125 (2017); <https://doi.org/10.1149/2.0281711jss>
- [15] P. Kordos et al, *Microelectronics Journal* 36, 438 (2005); <https://doi.org/10.1016/j.mejo.2005.02.040>
- [16] S. Faramehr, P. Igiü, and K. Kalna, *Modeling and Optimization of GaN Capped HEMTs. 10th International Conference on Advanced Semiconductor Devices and Microsystems (ASDAM), IEEE* (2014); <https://doi.org/10.1109/ASDAM.2014.6998668>
- [17] L. Yang, W. Mao, Q. Yao, Q. Liu, X. Zhang, J. Zhang, Y. Hao, *J. Appl. Phys.* 109, 024503 (2011); <https://doi.org/10.1063/1.3533984>
- [18] L. Wang, F. M. Mohammed, B. Ofuonye, I. Adesida, *Appl. Phys. Lett.* 91, 012113 (2007); <https://doi.org/10.1063/1.2754371>
- [19] C. Wood, D. Jena, *Polarization Effects in Semiconductors: From Ab Initio Theory to Device Applications*, Springer, New York, (2008); <https://doi.org/10.1007/978-0-387-68319-5>
- [20] O. Ambacher, J. Smart, J. R. Shealy, N. G. Weimann, K. Chu, M. Murphy, W. J. Schaff, L. F. Eastman, *J. Appl. Phys* 85(6), 3222 (1999); <https://doi.org/10.1063/1.369664>
- [21] Pu. Jinrong, S. Jiuxun, Z. Da, *Physics of Semiconductor Devices* 45(9), 1205 (2011); <https://doi.org/10.1134/S1063782611090107>
- [22] O. Ambacher, J. Majewski, C. Miskys, A. Link, M. Hermann, M. Eickhoff, M. Stutzmann, F. Bernardini, V. Fiorentini, V. Tilak, B. Schaff, L. F. Eastman, *J. Phys. Condens. Matter.* 14, 3399 (2002); <https://doi.org/10.1088/0953-8984/14/13/302>
- [23] Madhulika, A. Malik, N. Jain, M. Mishra, S. Kumar, D.S. Rawal, A.K. Singh, *Superlattices*

- and Microstructures 152, 106834 (2021); <https://doi.org/10.1016/j.spmi.2021.106834>
- [24] R. Kumar, S. K. Arya, A. Ahlawat, Inter. Journal of design & Communication Systems 4(2), (2013); <https://doi.org/10.5121/vlsic.2013.4205>
- [25] M. Guo, Z. Y. Guo, J. Huang, Y. Liu, S.Y. Yao, Chin. Phys. B 26, 028502 (2017); <https://doi.org/10.1088/1674-1056/26/2/028502>
- [26] S. Khandelwal, T. A. Fjeldly, Solid State Electronics 76, 60 (2012); <https://doi.org/10.1016/j.sse.2012.05.054>
- [27] S. M. Sze, K. K. Ng, Physics of Semiconductor Devices, Third Edition., John Wiley and Sons, Canada, (2007); <https://doi.org/10.1002/0470068329>
- [28] D. Godwinraj, H. Pardeshi, S. K.Pati, N. Mohankumar, C. K. Sarkar, Superlattices and Microstructures 54, 188 (2013); <https://doi.org/10.1016/j.spmi.2012.11.020>
- [29] Z. Wen et al, IEEE Transactions on Microwave Theory and Techniques 65(12), 5113 (2017)' <https://doi.org/10.1109/TMTT.2017.2765326>
- [30] T. R. Lenkaa, G. N. Dashb, A. K. Panda, International Conference on Solid State Devices and Materials Science, Physics Procedia 25, 36 (2012).
- [31] Ambacher O, Foutz B, Smart J, Shealy JR, Weimann NG, Chu K, et al, J Appl Phys 87, 334 (2000); <https://doi.org/10.1063/1.371866>
- [32] P. Gangwani, R. Kaur, S. Pandey, S. Haldar, M. Gupta, R. S. Gupta, Superlattices and Microstructures 44, 781 (2008); <https://doi.org/10.1016/j.spmi.2008.07.004>
- [33] A. Bellakhdar, A. Telia, L. Semra, A. Soltani, Proc. 24th Intern. Conf. Microelectronics -ICM 2012-, Dec. 17-20 , Algiers, Algeria (2012).
- [34] A. Bellakhdar, A. Telia, L. Semra, A. Soltani, International Conference on Engineering and Technology (ICET2012), Oct 10-11. New Cairo City, Egypt(2012).
- [35] K. Ahmeda et al, Microelectronics Reliability 115,113965 (2020); <https://doi.org/10.1016/j.microrel.2020.113965>
- [36] M. Shafiqul Islam, A. Ahad, H. Ahmed, S.Islam, 10th International Conference on Electrical and Computer Engineering (ICECE), 20-22 Dec, 2018, Dhaka, Bangladesh (2018).